

RESEARCH

Open Access



# The prognostic significance of circulating tumor cell enumeration and HER2 expression by a novel automated microfluidic system in metastatic breast cancer

Liye Wang<sup>1,4†</sup>, Ruoxi Hong<sup>1†</sup>, Simei Shi<sup>1†</sup>, Shusen Wang<sup>1</sup>, Yong Chen<sup>6</sup>, Chao Han<sup>5\*</sup>, Mei Li<sup>3\*</sup> and Feng Ye<sup>2\*</sup>

## Abstract

**Background** The prognostic value of circulating tumor cells (CTCs) in metastatic breast cancer (MBC) has been extensively studied and verified by the CellSearch<sup>®</sup> system. Varieties of microfluidic systems have been developed to improve capture efficiency with the lack of standardization and automation. This study systematically verified the positive threshold for prognosis and its guidance value in anti-HER2 therapy based on a novel automated microfluidic system OmiCell<sup>®</sup>.

**Methods** CTCs isolation, enumeration and labeling were performed using the OmiCell<sup>®</sup> system. CTCs identification and reporting were performed using the DeepSight<sup>®</sup> scanning system.

**Results** The capture efficiency and specificity of OmiCell<sup>®</sup> system was 91.9% and 90%, respectively. Then, 65 MBC patients with known HER2 status of their metastatic tumors were enrolled. In the cohort, we detected  $\geq 1$  CTCs in 59 patients (90.8%, range: 1–55 CTCs, median = 6),  $< 8$  CTCs in 45 (69.2%) and  $\geq 8$  CTCs in 20 (30.8%) patients at baseline. The patients with  $< 8$  CTCs had longer PFS than  $\geq 8$  CTCs (median, 7 vs. 4.4 months,  $p = 0.028$ ). CTC enumeration was found to be an independent prognostic factor in our cohort. Moreover, we found a weak concordance between tissue HER2 (tHER2) status and the corresponding CTCs ( $k = 0.16$ ,  $p = 0.266$ ). The patients with tHER2 positive and cHER2 negative had better PFS compared with patients with both tHER2 and cHER2 positive (median, 8.2 vs. 3.3 months,  $p = 0.022$ ).

**Conclusions** This clinical study shows the prognosis value of a new threshold of CTC number and meanwhile the guidance value of cHER2 status in anti-HER2 therapy.

**Keywords** Microfluidic device, Circulating tumor cells isolation, Human epidermal growth factor receptor 2, Prognostic, Clinical verification

<sup>†</sup>Liye Wang, Ruoxi Hong and Simei Shi contributed equally to this work.

\*Correspondence:

Chao Han

chao.han@afbio.cn

Mei Li

limei@sysucc.org.cn

Feng Ye

yefeng@sysucc.org.cn

Full list of author information is available at the end of the article



## Introduction

Circulating Tumor Cells (CTCs) are tumor cells shedding from primary or metastatic lesions which are responsible for tumor metastasis [1, 2]. CTCs represent the most complete carrier of tumor properties, including genomes, transcriptomes, proteins, phosphorylation patterns, etc. As a non-invasive method, CTC-based liquid biopsy exhibits important values for cancer diagnosis and future precision medicine [3]. The prognostic values of CTC detection by using CellSearch<sup>®</sup> platform have been documented as strong evidence in various cancers [4, 5]. However, the heterogeneity of CTCs, mainly manifested in the loss of epithelial phenotype through Epithelial-Mesenchymal Transition (EMT), leads to incomplete capture of CTCs by Cellsearch<sup>®</sup>, which is based on Epithelial Cell Adhesion Molecule (EpCAM)-positive immunoselection [6]. To overcome this limitation, different strategies have been proposed. The combination of antibodies targeting multiple antigens has been used to partially overcome the lack of specificity of current tumor markers [7]. Another approach is negative isolation by using a specific marker CD45 to remove all the leukocytes [8]. On the other hand, the label-free methods which are based on physical characteristics of CTCs such as size [9], deformability [10], density [11], and dielectrophoresis [12], can detect a larger spectrum of CTCs including those undergoing EMT transitions [9, 13, 14]. Recent progress in combination with these strategies has shown the advantages of using microfluidic techniques in CTCs detection due to its high precision in flow control [15, 16]. However, this technique is often limited in throughput, and pretreatment of blood samples, including centrifugation, red blood cell lysis, etc., is generally required before CTC capture.

To improve the filtration efficiency, we previously developed a new type of filter consisting of an array of conical-shaped holes that facilitate the passage of blood cells but the retention of captured CTCs under microfluidic conditions [17]. A microfluidics-based automatic enrichment system in clinical practice [18] has shown rapid, reliable, and reproducible results, benefiting from the automation. Also in order to increase the reliability and repeatability of this new filter with conical shape [17], we developed a system for automatic and multi-sample analysis to reach a more reliable stage for clinical and future applications. More specifically, this system (including OmiCell<sup>®</sup> and DeepSight<sup>®</sup>) has been designed for fully automatic and parallel processing, starting from blood sample injection to multi-color immunostaining, of up to 8 blood samples without any human intervention. Accordingly, a dedicated imaging system has been developed for advanced CTC classification and protein expression status assessment. Together, the CTC platform is

able to isolate more CTC phenotypes, including both epithelial and mesenchymal CTCs as well as cancer stem cells. This platform is also capable to identify different types of cell clusters, including cancer associated fibroblast, CTC-neutrophils clusters, CTC-platelets, which are all important for understanding the tumor metastasis mechanism. Compared to affinity-based methods, this platform should be more appropriate for analyses of tumor heterogeneity, tumor drug resistance, etc. Compared to other filtration-based systems, this platform has been optimized in terms of filter design, microflow control, throughput, and fully automatic processing. Finally, this platform is robust, easy to use, and compatible to downstream analyses of the isolated CTCs.

The aim of this work is to study the performance of this platform in CTC detection in metastatic breast cancer (MBC). As a heterogeneous disease, several studies have shown that substantial discrepancy of human epidermal growth factor receptor-2 (HER2) status exists between primary and recurrent/metastatic tumors in breast cancer [19, 20]. In addition to CTC enumeration, considerable research has been focused on the HER2 status of CTCs, showing a [21, 22] large inconsistency of HER2 status between CTC and tumor tissue [21, 23–29]. The clinical implication of this problem in anti-HER2 therapy has been further studied, confirming the significance of this inconsistency [25, 28, 30, 31]. Previously studies have also shown that HER2-negative primary tumors were capable to acquire HER2 amplification during disease progression [28, 30]. It is therefore important to develop a more systematic study on heterogeneity and correlation between tissue and CTC HER2 status in MBC patients.

After presenting the new platform and the results of assessment on sensitivity, specificity and limit of detection, blood samples taken from MBC patients were analyzed. We found that CTCs represent an independent predictor of outcome in patients with MBC patients. By analyzing the HER2 expression status in CTCs, we also found that the consistency of the HER2 status between tissue and CTCs was correlated with prognosis in MBC patients. Further clinical trial including a larger cohort is warranted to validate the clinical value of CTC analyses using this platform.

## Materials and methods

### Study design and participants' enrollment

MBC patients with known HER2 status of their metastatic tumors were enrolled. Previous systemic treatment (s) for metastatic disease were allowed. For these patients, baseline CTCs evaluations have been done at the time point that an interval > 2 weeks after the last systemic treatment. For CTC enumeration, peripheral blood samples (5 mL) were collected from all participants

(patients and healthy donors) using an indwelling sheathe syringe needle on the day before the system treatment and collected in a collected into EDTA tube. All samples were processed within 24 h.

All patients signed an informed consent to participate in the study, which was approved by the Ethics Review Committees (ERC) of Sun Yat-sen University Cancer Center, Guangzhou, China. All the experimental protocols, including patient recruitment, blood collection, CTC isolation, staining and imaging processing, and tissue pathological tumor characterization were approved by the local ethical board (B2021-062).

#### Cell lines and culture

Different cancer cell lines MCF-7, ZR-75-1, MDA-MB-361 and SKBR3 were purchased from the Typical China Academy Culture Collection Commission Cell Library (Shanghai, China). The cell lines were cultured in high glucose RPMI-1640 medium supplemented with 10% fetal bovine serum, 100 units/mL penicillin and 100  $\mu\text{g}\cdot\text{mL}^{-1}$  streptomycin (Invitrogen) in a cell culture incubator at 5% CO<sub>2</sub> and 37 °C ambient temperature. Cells were cultured to 70–90% confluence then lifted with 0.05% trypsin–EDTA (Invitrogen) and spun down once at ~100 rcf in preparation for different purpose experiments.

#### Workflow of OmiCell® system for CTC detection

The OmiCell® system is a high precision and highly sensitive CTC detection platform which is designed for whole working flow automation and standardization from CTC enumeration to labelling. DeepSight® scanning system is an automatic highly sensitive and multi channels fluorescence characterization and analyzing platform developed for CTC identification and reporting. Briefly, CTC isolation, enumeration and labeling were performed using the OmiCell® system, CTC identification and reporting were performed using the DeepSight® scanning system. Regarding the preservation of blood samples, 5 ml of peripheral blood was stored in ethylenediaminetetraacetic acid (EDTA) collection tubes, transported at room temperature to the laboratory, and processed for analysis within 6 h of collection.

For CTC isolation and labelling with OmiCell® system, firstly, the microfluidic device with filter is inserted in the chip holder of the machine, clamped by pressure and connected with corresponding connectors prior working flow begin. 5 ml blood samples was prepared by mixing with manufacturer (Anfang Biotech, Guangzhou, China) prepared buffer at a ratio of 1:1 and incubated at room temperature for 10 min. After loading diluted blood samples in the reservoir on the chip and starting the system, the CTC enumeration and immunofluorescence labelling

process will be performed automatically in chip until the whole working flow is finished. During CTC enumeration, blood samples will be filtrated at optimized flow rate by the system. After filtration, the membrane surface was washed for multi times with PBS solution before immunofluorescence steps. During the immunofluorescence staining steps, cells on membrane was fixed, permeabilized and blocked with corresponding reagents delivered automatically by the dispenser through the reservoir. Then, the antibodies cocktail was added and incubated which include FITC labeled anti-Pan CK (FITC) (AE1/AE3, Mouse monoclonal antibody, Thermo Fisher Scientific, Cleveland, OH, USA), Cy7 labeled anti-CD45 (HI30, Mouse monoclonal antibody, Thermo Fisher Scientific, Cleveland, OH, USA) and DAPI for cell nuclear staining. Detected CTCs were defined as nucleated (DAPI+, Thermo Fisher Scientific, Cleveland, OH, USA) intact cells with positive CK and negative CD45. Additional antibody such as PE labeled anti-HER2 (EPR19547-12, Rabbit monoclonal antibody, Abcam, UK) could be added to for HER2+CTC characterization. Finally, the chip and filter were taken out, the filter was mounted on cover slide which is ready for later microscope scanning, CTC identification and reporting. The whole working flow schema is presented in Fig. 1.

For CTC identification and reporting with DeepSight® scanning system, firstly, the mounted filter on the cover slide prepared was loaded on the stage. After initialization and setting, the system began to scan each area of the filter. In each area, the scanning system will focus, change optic filter and take images automatically. A 10X magnification objective was used for screening here. In addition, CTC identification process was performed simultaneously during scanning by figuring out selected CTC on the software interface. A deep learning network “ResNet-18” [32] was developed to precise segmenting cell edge, to extract and quantified all necessary cell features for identification such as size, shape, marker intensity, Signal–Noise-Ratio (SNR), etc. Considering quantified features and threshold, detected CTCs were defined as nucleated (DAPI+) intact cells with a diameter > 5  $\mu\text{m}$  which is labeled with Pan CK+ and CD45-. When anti-HER2 antibody was added, from the preliminary selected CTC according with the defined criteria, HER2+CTC could also be classified which was defined as DAPI+, PanCK+, CD45-, and HER2+ cells (the PanCK-/HER2+ cells are not considered as CTC here). Further accurate classification is further performed by a deep learning network “ResNet-18” [32] with annotated CTC dataset, more quantified CTC morphology and fluorescent biomarker expression pattern characteristics could be evaluated. Through deep learning algorithms, typically no more than 300 candidate CTCs are ranked

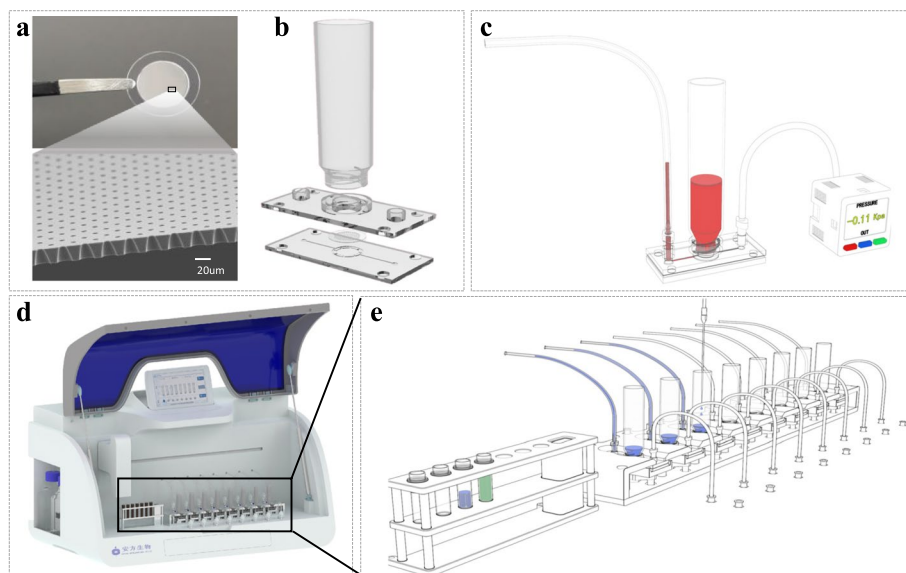


**Fig. 1** Overview of the OmiCell<sup>®</sup>. **a** Image of a filter with conical shaped via holes. **b** Photograph of a filter integration microfluidic device. **c** Schematic representation of pressure monitoring during aspiration of a blood sample from the outlet of the device (left). **d** Photograph of the system. **e** Schematic representation of the multi-sample processing configuration. Staining reagents are transported from tubes (left) to the sample reservoirs (right) with a tiny needle after filtration, all being processed automatically with optical parameters and minimal reagents

in order of confidence. The entire analysis time, including image segmentation, screening, and deep learning analysis, completed within 30 min. When confirming CTCs, the physician can click on each candidate CTC in the software. The high-precision motorized stage will position the selected candidate CTC in the center of the microscope field of view for the physician to review under a microscope. Finally, the system will generate a report with all CTC identified and classified. The whole working flow schema is presented in Fig. 2.

#### Performance validation of OmiCell<sup>®</sup> system

In the following validation, SKBR3 cell lines were digested, harvested and stained with the fluorescent dyes-5  $\mu\text{g}/\text{ml}$  of Hoechst 33,342 (Beyotime) and 5  $\mu\text{m}$  Dil (Beyotime). Cells were counted with a manual counting slide (Watson) and then diluted with PBS to ensure  $\sim 50$  cells in 100  $\mu\text{L}$  of PBS, then certain number of cells were picked using a 10  $\mu\text{L}$  pipette under an inverted microscope (Leica) at the  $\times 20$  objective and spiked into 5 mL blood collected from healthy donors. The spiked in cells were processed by OmiCell<sup>®</sup> and DeepSight<sup>®</sup> system.

The degree of sensitivity of the instrument's output to changes in the input is referred to as sensitivity, while the degree of linearity between the instrument's output and the input is referred to as linearity. Varying number of Cells from 5 to 1000 in 6 grades were spiked in peripheral blood from healthy donors. The sensitivity is taken the linearity of recovery rate (=number of cells recovered/

number of cells spiked \*100%), where assay linearity was evaluated by plotting the actual Cell number recovered versus the spiked cell number for each of the concentrations tested, the corresponding correlation coefficient  $r$  was calculated.

Limit of detection (LOD) is the lowest concentration of tumor cells detectable. 3, 2, and 1 cell were accurately picked for test, the LOD is defined as the minimal spiked Cell number when the detectable rate of CTC > 80% among 20 times repeated experience. The specificity is defined as the percentage of negative samples among the 20 samples, 5 mL blood collected from 20 healthy donors were processed by standard protocol (Sect. "Workflow of OmiCell<sup>®</sup> system for CTC detection", "Performance validation of OmiCell<sup>®</sup> system").

Repeatability was measured by calculating the percent coefficient of variation (%CV) of recovery rate (20 cells) evaluated across 3 separate days by two operators using paired blood samples, tests repeat for 5 time for each operator and each day.

#### Threshold determination of HER2-positive CTC

HER2 positive threshold of CTCs was calibrated through peripheral blood spiking experiments with different HER2 expression level cell lines. As proposed by other studies [25], MCF-7, ZR-75-1, MDA-MB-361 and SKBR3 cell lines were prepared as models whose HER2 status were classified as 0, 1+, 2+, 3+, respectively. For HER2 intensity determination, 5 ml of peripheral blood

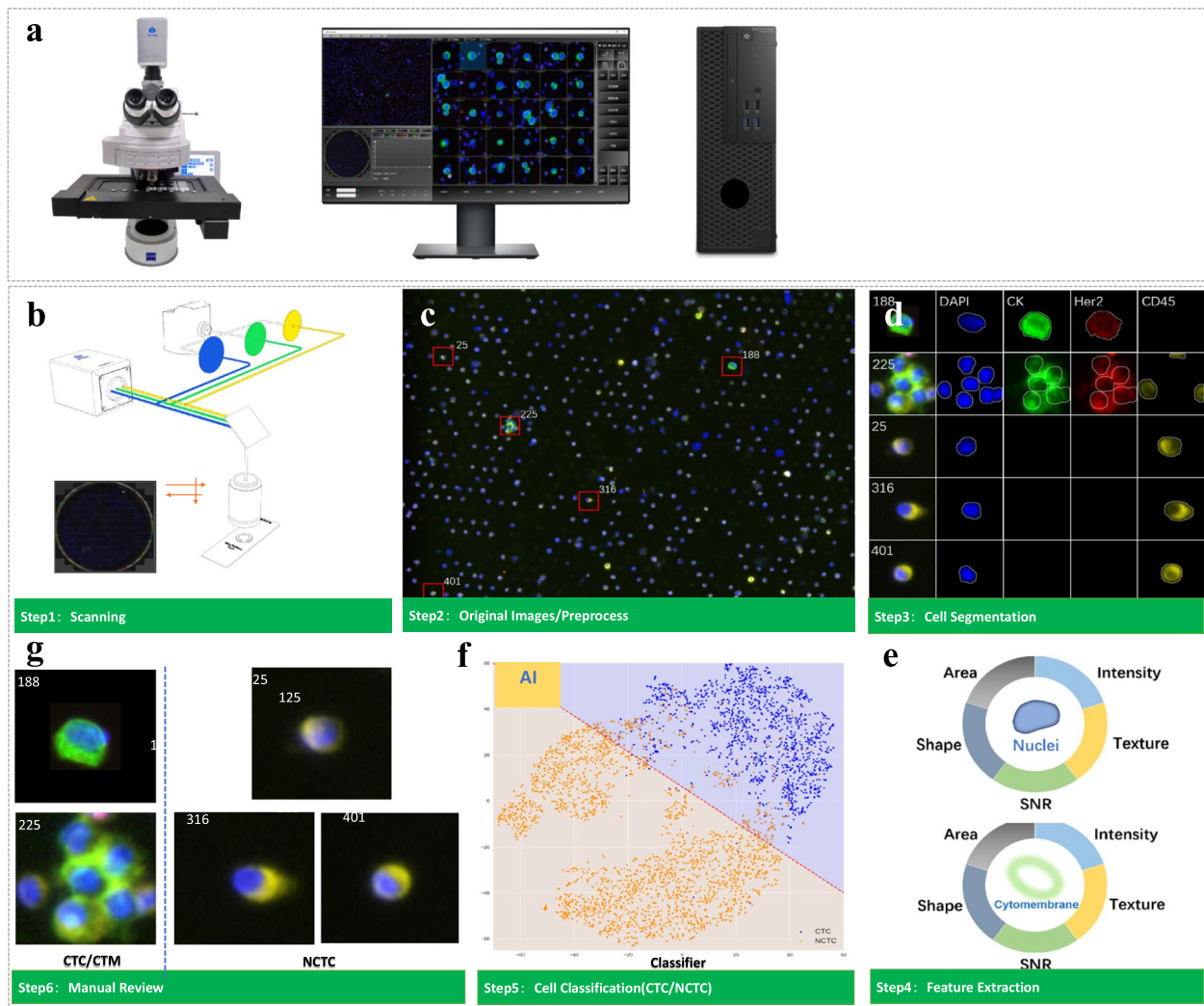


**Fig. 2** Overview of the DeepSight<sup>®</sup>. **a** Photograph of the system, including an optical microscope with autofocus and multi-sample scan stage. **b** Schematic representation of the imaging sub-unit. **c** The merge image of multiple fluorescence in one image field. **d** Contour extraction for all cell under each fluorescence channel. **e** Extract features (Area, Intensity, Texture, Area and Shape etc.) within the contours of each nucleus and cytoplasm separately. **f** Use a trained deep learning network “ResNet-18” to classify CTC and nCTC and **(g)** the final result was confirmed by pathologists

from a healthy donor were spiked with approximately 500 cells from these cell lines and then processed with Omi-Cell<sup>®</sup> system and DeepSight<sup>®</sup> system by using the same protocol described above. The average mean intensity of each cell line has been characterized.

The cut-off of HER2 positive was according to the expression of BC cell lines. Among them, MCF-7 was HER2 negative, the mean intensity was 1.9, ZR-75-1 was HER2 1+, the mean intensity was 2.8. Considering that

the protein expression of CTCs is typically lower than that of established cell lines, we have opted to use a ratio of 2.5 as a more appropriate threshold for determining HER2 positivity, consistent with the standards utilized in the literature [23]. Therefore, HER2-positive CTCs were defined as CTCs with HER2 immunofluorescence intensity that was at least 2.5 times greater than the background in tests using BC cell lines [33]. Its formula for assessing HER2 intensity on CTC was:

$$\text{HER2 Intensity} = \frac{\text{Foreground Intensity (Cell HER2 staining)} / \text{Surface Area}}{\text{Background Intensity} / \text{Surface Area}}$$

**Table 1** Description of characteristics in analytical validation

Performance Characteristics	Spike-In CTCs	Assessment Parameter	Result
Capture rate	5 ~ 1000 CTCs spiked in peripheral blood from healthy donors	Linearity of recovery rate of detected cell numbers	91.9% ( $R^2 = 0.99$ )
Linearity		Linear Regression of detected CTCs	
Limit of detection (LOD)	1–3 CTCs spiked in peripheral blood from healthy donors, repeat for 20 times	Lowest measurable CTC count with >80% successful rate	2 CTC /5 ml
Specificity	Peripheral blood from 20 healthy donors	False-positive detection rate	90%
Repeatability	20 CTCs Spiked in peripheral blood from healthy donors with processed by 2 operators in 3 days, repeat for 5 times	Intra-assay and inter assay variability calculated by coefficient of variation (%CV)	6.3% for Operator A and 6.8% for Operator B

Briefly, HER2-positive CTCs could also be classified which was defined as DAPI+, PanCK+, CD45-, and HER2+ cells (the PanCK-/HER2+ cells are not considered as CTC here).

**Statistical analysis**

The demographic data and clinicopathologic features were collected retrospectively. Progression-free survival

(PFS) was calculated from the date of baseline CTC assessment to the date of definite diagnosis of disease progression, death, or date of last follow-up. We used X-tile software (V.3.6.1; Yale University, New Haven, Connecticut, USA) to calculate the optimal cut-off value for CTCs when PFS was defined as status variable. The associations between the CTCs and clinicopathological variables were analyzed using the  $\chi^2$  test or Fisher’s exact

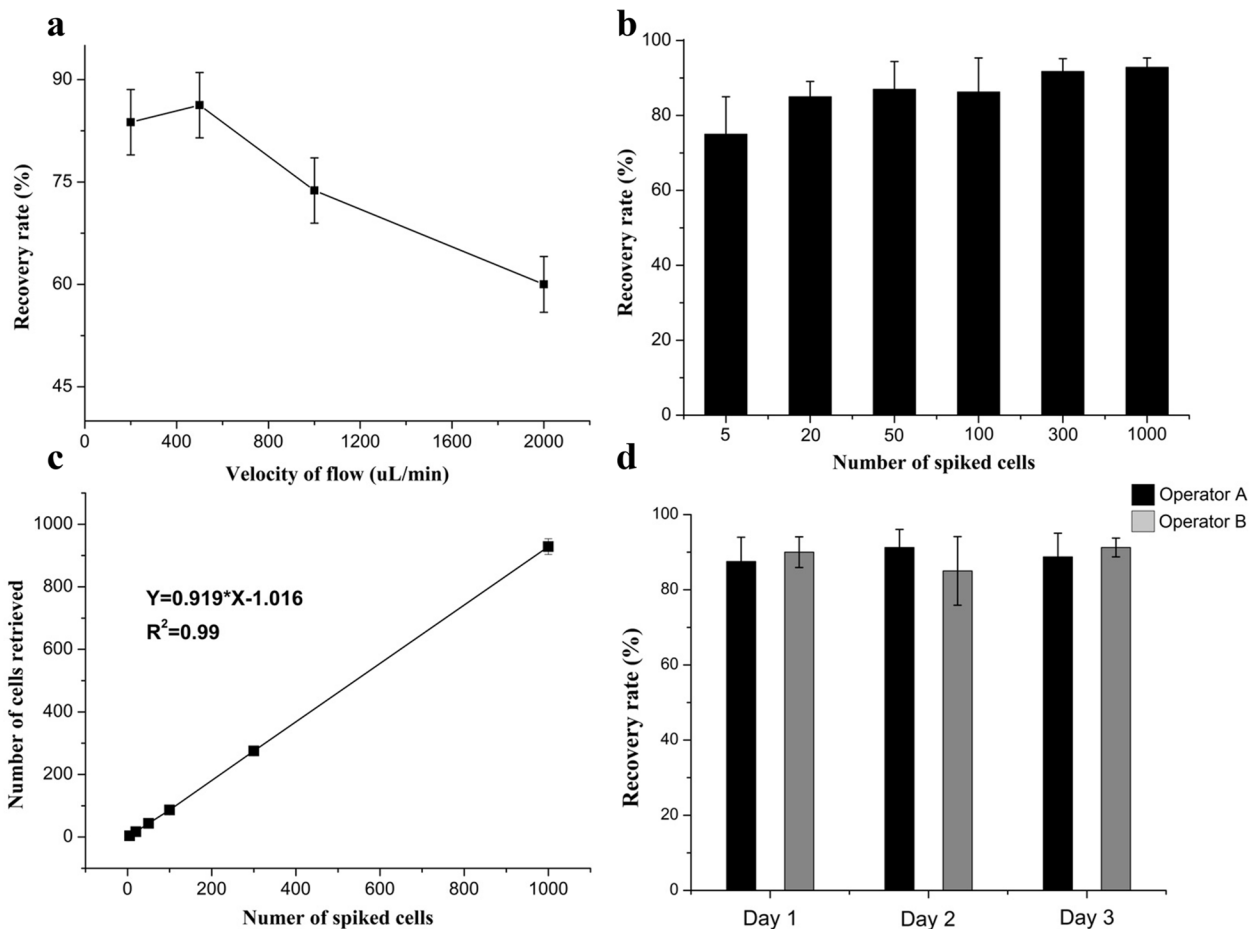


**Fig. 3** Performance of the platform. **a** Recovery rate as a function of flow rate for SKBR3 cells spiked in blood. **b** Average recovery rate for SKBR3 cells spiked in blood with cell number in the range of 5 to 1000. **c** Linear regression of average recovery rate with spiked cell number, **(d)** Average recovery rate by two operators during 3 days

test. Cohen's Kappa and 95% confidence intervals (CI) was used to assess agreement on HER2 status between metastatic tumor and CTCs. The Kaplan–Meier method was used to estimate PFS, and differences were compared using the log-rank test. Hazard ratios (HRs) were calculated using univariate Cox regression analysis. Multivariate Cox regression analysis was performed to test the independent significance of different factors. Significant variables ( $p < 0.05$ ) in univariate analysis were subjected to the multivariate analysis. Data were analyzed by using SPSS 26.0 software, and the graphs were profiled by using GraphPad Prism 8.4.0. All statistical tests were two sided and considered significant when the  $p$  value  $< 0.05$ .

## Results

### Analytical performance of OmiCell® system

The capture rate, linearity, LOD, specificity and repeatability of OmiCell® system revealed by spiking tests were shown in Table 1.

We observed the capture efficiency exhibit a peak when the flow rate is around 500ul/min, then it decreases with the flow rate increasing, which is shown in Fig. 3(a). The capture efficiency (when the spiked cell number is 20) under each flow rate are shown in Supplementary Table 1. Considering the long filtration time may cause the problem of blood coagulation and cell morphology change, we set the flow rate as 500ul/min.

The sensitivity of the system is 91.9% with a correlation coefficient  $R^2 = 0.99$ , taken as the linear regression of average recovery rate (Fig. 3(b) (c) and Supplementary Table 2). The results of the LOD evaluation test were summarized in Supplementary Table 3, indicating that the LOD is 2 CTC /5 ml blood sample. For specificity test, the results manifested that the system specificity is 90%. We detected CTC in 2/20 healthy donor samples (N3 and N15), indicating a low false positive rate of our system (shown in Supplementary Table 4). To better characterize the repeatability of the platform, the coefficient of variation (% CV) of the recovery rate was evaluated across 3 separate days ( $n = 3$ ) by two operators ( $n = 2$ ) using paired blood samples. The results of these intra- and inter-assays showed high repeatability with the calculated % CVs were 6.3% for Operator A and 6.8% for Operator B (Fig. 3(d) and Supplementary Table 5).

### Patient characteristics and blood samples

We enrolled 65 patients with MBC from September 2020 to March 2021. Patients were followed up to August 2021. The median follow-up time was 5.9 months. At the end of follow-up, 44 (67.7%) patients had disease progression and no patients died from MBC. Characteristics of the 65 MBC patients enrolled in the study were summarized in

Table 2. The mean age of all these patients was 45.4 years (range 29 to 69 years). 44 patients (67.7%) were premenopausal at diagnosis, and 32.3% of them were postmenopausal. By assessing immunohistochemistry of metastatic

**Table 2** Patient characteristics

Variable	Result $n = 65$ (n%)
Median age, years (range)	41.5 (29–69)
Menopausal status	
Pre-menopausal	44 (67.7)
Post-menopausal	21 (32.3)
ER status <sup>a</sup>	
Negative	21 (32.3)
Positive	44 (67.7)
PR status <sup>a</sup>	
Negative	22 (33.8)
Positive	43 (66.2)
HER2 status <sup>a</sup>	
Negative	45 (69.2)
Positive	20 (30.8)
Subtype <sup>a</sup> (based on receptor status)	
Luminal A	3 (4.6)
Luminal B	46 (70.8)
HER2-positive	4 (6.2)
Triple-negative	12 (18.5)
Metastatic site	
Bone	34 (52.3)
Visceral	36 (55.4)
Both	19 (29.2)
Number of metastatic sites	
One site	11 (16.9)
Multiple sites	54 (83.1)
Therapeutic setting	
First line	43 (66.2)
Second line	9 (13.8)
≥ Third line	13 (20.0)
Sample taken at	
Initial diagnosis	16 (24.6)
Progression from previous palliative therapy	37 (56.9)
During treatment	12 (18.5)
Treatments	
Chemotherapy	57 (87.7)
Endocrine therapy	12 (18.5)
Targeted therapy	22 (33.8)
Immune checkpoint inhibitor	14 (21.5)
Unknow	2 (3.1)
CTC positivity <sup>b</sup>	
< 8 cells	45 (69.2)
≥ 8 cells	20 (30.8)

<sup>a</sup> ER, PR, HER2 status and subtype of the metastatic tumor; <sup>b</sup>CTC at baseline. ER, estrogen receptor; PR, progesterone receptor; HER2, human epidermal growth factor receptor 2; CTC, circulating tumor cell

tumor, there were 44 (67.7%) ER-positive patients, 43 (66.2%) PR-positive and 20 (30.8%) HER2-positive, respectively (Supplementary Table 6). In the 65 patients, 3 (4.6%) were Luminal-A subtype, 46 (70.8%) were Luminal-B subtype, 4 (6.2%) were HER2-positive and 12 (18.5%) were triple-negative subtype, as indicated by IHC results of metastatic lesions (Supplementary Table 6). Among them, 34 patients (52.3%) had bone metastasis, 36 (55.4%) had visceral metastasis such as pulmonary or hepatic metastasis (Supplementary Table 7). For all enrolled MBC patients, blood samples were taken at baseline and as longitudinal follow-up samples in 40 cases. The baseline samples were taken at initial diagnosis ( $n=16$ , 24.6%), after disease progression from previous palliative therapies and before the start of a new treatment regimen ( $n=37$ , 56.9%) and during therapy ( $n=12$ , 18.5%).

**CTCs enumeration in MBC and its prognosis value**

We detected  $\geq 1$  CTCs in 59 out of 65 samples at baseline (90.8%, range: 1–55 CTCs, median=6) (Fig. 4a). 2 to 4 months after baseline, we detected  $\geq 1$  CTCs in 34 out of 40 samples (85%, range: 1–58 CTCs, median=6). By using the X-tile software, we found that the optimal cut-off value of baseline CTC count that correlated with PFS was 8. In our cohort, 45 (69.2%) patients had  $< 8$  CTCs and 20 (30.8%) had  $\geq 8$  CTCs at baseline. The association between baseline CTC count and clinicopathological variables was demonstrated in Table 3. No significant difference was found between the group of  $CTC \geq 8$  or  $< 8$ . Survival analysis was performed on 61 patients (4 patients were lost to follow-up). We found that 27 patients (64.3%) in  $< 8$  CTCs group and 17 patients (89.5%) in  $\geq 8$  CTCs group had progressive disease (PD).

We further evaluated the prognostic value of CTC enumeration in our cohort. As shown in Fig. 4b, the patients with  $< 8$  CTCs had longer PFS than patients with  $\geq 8$  CTCs (median, 7 vs. 4.4 months, 95% CI 0.87–2.92;  $p=0.028$ , hazard ratio (HR): 1.93, 95% CI 0.97–3.84). In the cox multi-variate analysis of the correlation between clinicopathological characteristics and PFS,  $CTC \geq 8$  or  $< 8$  was also found to be independently predictive of PFS (Table 4).

**cHER2 statues in MBC and its dynamics during the treatment**

In the current study, a CTC-HER2 (cHER2) positive case was defined by  $> 50\%$  of CTCs detected in 5 ml blood over-expressing HER2. A tumor HER2 (tHER2) positive case was defined as HER2 (3+) assessed by IHC or FISH in metastatic tumor tissue, in accordance with the ASCO/CAP guideline for HER2 testing [34]. At baseline, out of the 65 MBC patients, the proportion of HER2 positive CTCs ranges from 0 to 100%. Among them, 29 patients were defined as cHER2 positive. After treatment, 32 patients participated in the CTC test, and 22 patients were defined as cHER2 positive, the proportion of cHER2 positive patients increased significantly after treatment. Meanwhile, 20 of 22 patients’ cHER2 status changed before and after treatment, demonstrating the high frequency of dynamic changes of cHER2, as shown in Fig. 5.

**Discordance of HER2 status between CTCs and tumor tissue**

From the 65 patients with MBC, in 48 cases a tissue sample from the metastatic lesion was available. Among tHER2-positive patients, 57.1% (8/14) were determined to be cHER2-negative. Among 34 tHER2

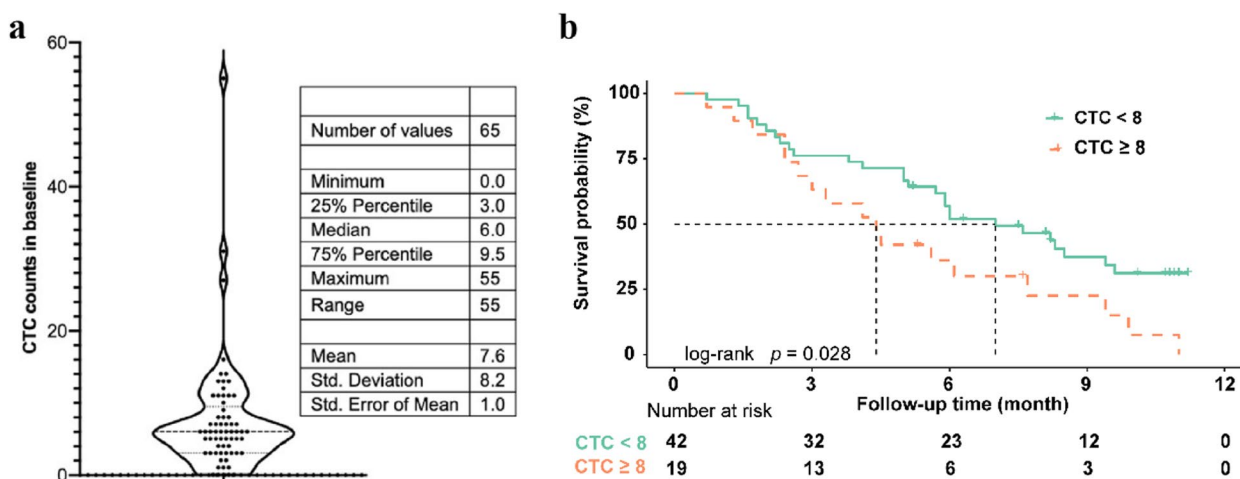


**Fig. 4** Statistics of CTCs and probability of survival of cancer patients. **a** Distribution of CTCs detected at baseline. **b** Progression-free survival (PFS) according to baseline circulating tumor cells (CTCs)



**Table 3** Association of CTC ( $\geq 8$  versus  $< 8$ ) with clinicopathological variables

Variable	CTC < 8 N=45 (%)	CTC $\geq 8$ N=20 (%)	p Value
Age at diagnosed (years)			0.15
$\leq 50$	34 (75.6)	11 (55.0)	
$> 50$	11 (24.4)	9 (45.0)	
Menopausal status			0.16
Pre-menopausal	33 (73.3)	11 (55.0)	
Post-menopausal	12 (26.7)	9 (45.0)	
ER status			1.00
Negative	15 (33.3)	6 (30.0)	
Positive	30 (66.7)	14 (70.0)	
PR status			1.00
Negative	15 (33.3)	7 (35.0)	
Positive	30 (66.7)	13 (65.0)	
HER2 status			0.26
Negative	29 (64.4)	16 (80.0)	
Positive	16 (35.6)	4 (20.0)	
KI67			0.58
$\leq 40$	21 (46.7)	11 (55.0)	
$> 40$	24 (53.3)	9 (45.0)	
Subtype (based on receptor status)			0.48
Luminal A	3 (6.7)	0	
Luminal B	30 (66.7)	16 (80.0)	
Triple-negative	8 (17.8)	4 (20.0)	
HER2-positive	4 (8.9)	0	
Metastatic site			0.93
Bone	10 (29.4)	5 (27.8)	
Visceral	11 (32.4)	7 (38.9)	
Both	13 (38.2)	6 (33.3)	
Number of metastatic sites			0.74
One site	9 (20.0)	3 (15.0)	
Multiple sites	36 (80.0)	17 (85.0)	
Therapeutic setting			0.60
First line	29 (64.4)	15 (75.0)	
Second line	7 (15.6)	1 (5.0)	
$\geq$ Third line	9 (20.0)	4 (20.0)	

negative patients, 26.5% ( $n=9$ ) were determined as cHER2 positive. In our cohort, only a weak concordance was found between tHER2 status and the corresponding CTCs ( $k=0.16$ ,  $p=0.266$ , 95% CI: -0.13 to 0.45).

#### cHER2 statute as a tool for predicting anti-HER2 therapy efficacy

The prognostic role of HER2 status discordance was explored in both tHER2 positive and negative groups. As shown in Fig. 6a, patients with tHER2 positive and cHER2 negative had better PFS compared with patients with both tHER2 and cHER2 positive (median, 8.2 vs.

3.3 months, 95% CI: (0.72 to 8.58);  $p=0.022$ , HR: 3.60, 95% CI: 0.80 to 16.19). Whereas in tHER2-negative patients, cHER2 status did not correlate with PFS (Fig. 6b). Survival analysis for the whole group stratified by tHER2 and cHER2 status indicated that patients with both tHER2 and cHER2 positive status had the most dismal prognosis (Fig. 6c).

#### Discussion

Nowadays, CTCs have been widely studied in both fundamental researches to investigate its role in cancer metastasis and clinical validity to discover its potential for cancer diagnosis and treatment. However, up to date, the clinical research data of CTC analyses that can be utilized to directly guide therapeutic decisions is still limiting. From the technology point of view, current methods for CTC enumeration cannot fully satisfy to capture and identify all CTC subtypes. For instant, the CellSearch system is the FDA approved technology which meet both requirements, but it is based on epithelial markers only, which fails to reflect all the potential subtypes of CTCs. Some automatic systems have been realized, but most efforts are concentrated only on CTC isolation. The Parsortix<sup>®</sup> PC1 system is a semi-automated, epitope-independent microfluidic device that captures rare cells based on size and deformability, offers reproducibly high capture efficiency [35]. CTC detection flow is complex which involves not only CTC enrichment but also staining, identification and reporting. In order to make the process stable, reproducible and with high throughput, each step is expected to be standardized because of the rarity of CTC. A whole process automatic and robust system is required to ensure the clinic practice.

Among the current CTC filtration technologies, the size-based method is perhaps the simplest, which relies mainly on the size and deformability differences between CTCs and blood cells. Considering different aspects of CTC detection including isolation, staining, identification, reporting and facility of downstream analyzing, we developed a whole working flow system OmiCell<sup>®</sup>. CTC capture and staining could be realized by using a microfluidic device with an integrated filter with conical-shaped micro-holes. The OmiCell<sup>®</sup> multi-channel system have been designed with the microfluidic device allowing automatic processing 8 samples parallel in one cycle with high precision flow rate and trans-filter pressure control. Once the blood sample is loaded, the system will process the sample until cell staining finished. Then, we developed the DeepSight<sup>®</sup> multi-channel scanning system which is composed with automatic scanning microscope and accurate image analyzing software powered with accurate algorithms considering multiple CTC features (such as size, marker expressions intensity, etc.). With

**Table 4** Cox regression analysis of the relationship between clinicopathological characteristics and progression-free survival

	Univariate			Multivariate		
	HR	95% CI	p Value	HR	95% CI	p Value
Age at diagnosed (years)						
≤ 50	1.00					
> 50	1.33	(0.71–2.49)	0.37			
Menopausal status						
Pre-menopausal	1.00					
Post-menopausal	0.98	(0.52–1.83)	0.95			
ER status						
Negative	1.00					
Positive	0.65	(0.35–1.22)	0.18			
PR status						
Negative	1.00					
Positive	0.62	(0.33–1.16)	0.13			
HER2 status						
Negative	1.00					
Positive	1.03	(0.55–1.95)	0.93			
KI67						
≤ 40	1.00			1.00		
> 40	2.41	(1.27–4.57)	<b>0.01</b>	3.02	(1.52–5.99)	<b>0.002</b>
Subtype (based on receptor status)						
Luminal A	1.00					
Luminal B	1.15	(0.27–4.83)	0.85			
Triple-negative	1.99	(0.43–9.24)	0.38			
HER2-positive	1.28	(0.21–7.68)	0.79			
Metastatic site						
Bone	1.00					
Visceral	2.44	(1.00–5.94)	0.05			
Both	1.58	(0.65–3.86)	0.32			
Number of metastatic sites						
One site	1.00					
Multiple sites	1.49	(0.93–2.38)	0.10			
Therapeutic setting						
First line	1.00					
Second line	1.68	(0.73–3.87)	0.22			
≥ Third line	1.62	(0.76–3.44)	0.21			
CTC positivity <sup>b</sup>						
< 8 cells	1.00			1.00		
≥ 8 cells	1.95	(1.06–3.61)	<b>0.03</b>	2.13	(1.04–4.38)	<b>0.04</b>

ER status, PR status, HER2 status, and Luminal A, Luminal B, Triple-negative molecular subtypes was performed based on the metastatic tumor profile

this system, we are able to scanning 8 filters one by one with automatic focusing, filter changing, capturing and reporting without any personal assisting. Our system can detect different CTC subtypes by the following scheme: 1) the OmiCell<sup>®</sup> platform can provide custom antibody loading area and program settings; 2) the DeepSight<sup>®</sup> platform will scan all the cell nucleus and then provide corresponding custom criteria for identification of

subtypes of CTCs. The performance of the two systems have been demonstrated by using a filter with conical-hole of small diameter 6.5 μm, a flow rate of 0.5 mL/min, and spiked tumor cell lines for in vitro studies, a capture efficiency as high as 91.9% could be reached. In addition, 90% specificity was obtained with healthy donor's blood. Remarkably, the sensitivity threshold could be down to a single cell. It is also highly desirable to collect the

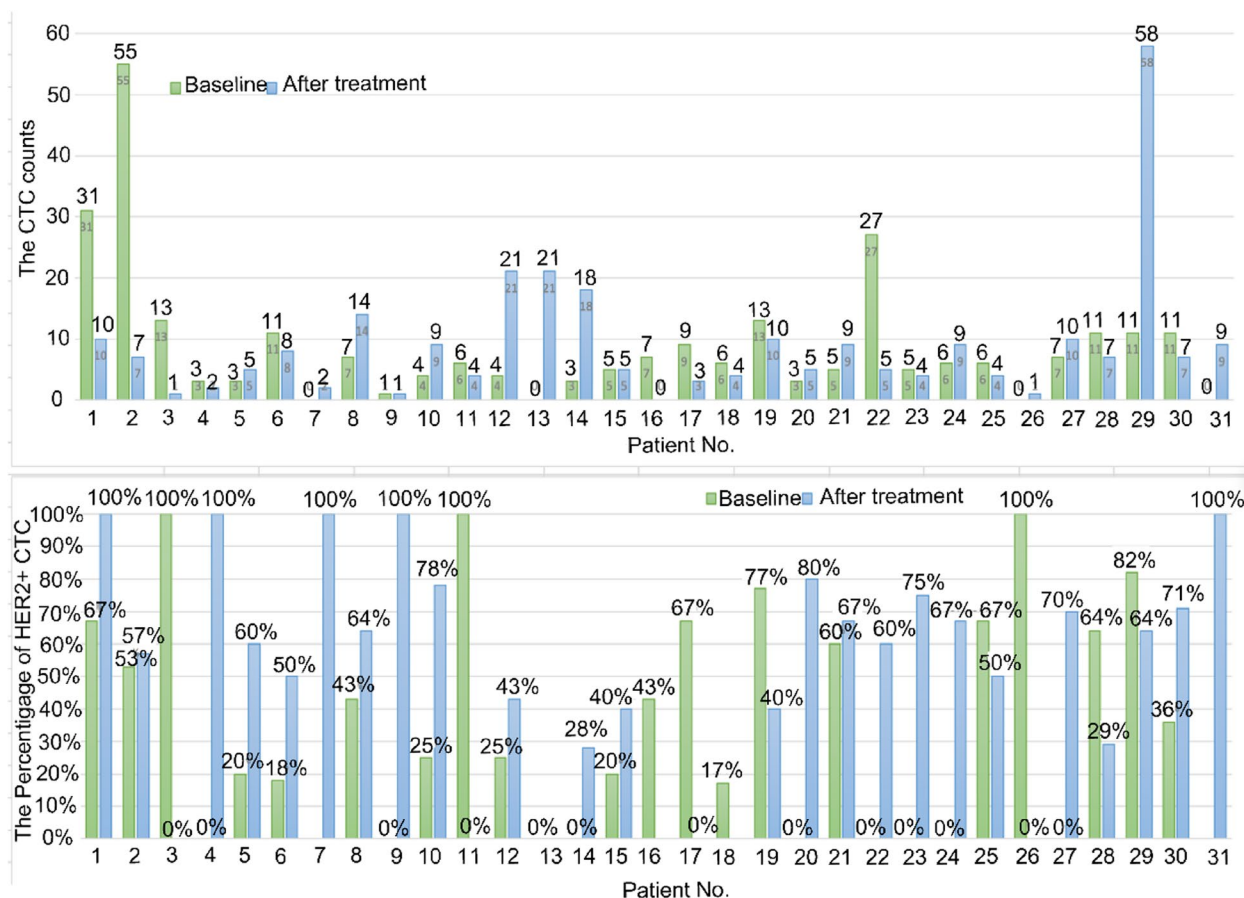


**Fig. 5** Comparison of CTC count and CTC-HER2 status changed before and after treatment

captured cells for downstream studies such as single-cell RNA-seq and genotypic analyses.

The prognostic role of CTC enumeration has the highest level of evidence in the clinical application of CTC analyses. Previous studies have established  $\geq 5$  CTCs per 7.5 ml of peripheral blood by CellSearch system as the threshold for poor prognosis in MBC [36]. While in the current study, we found a higher prognostic threshold of CTCs, which is  $\geq 8$  CTCs/5 ml blood as tested by our platform. This difference might be due to the higher numbers of CTC detected in our platform. The standardized conical hole integrated device, automated processing system and improved identification system could avoid CTC loss. These may contribute to the increase in the threshold of prognostic significance. The sensitivity of this system needs further verification through a larger cohort of study and longer follow-up time.

Previous studies have demonstrated that there are inconsistencies in HER2 expression between primary tumors and their metastases [37]. Alternatively, CTCs are shed from both primary site and metastases site,

which represent a global status and real-time phenotypes patients' tumors. Recent reports also indicate that there is a discordance of HER2 expressing between tissue and CTCs [21, 24, 26], which is in consistent with our research. Considering the HER2 status of CTCs maybe used as guidance for target therapy, it attracted a lot of research interests which could be summarized from two aspects. First, can tissue HER2 positive patients continue to benefit from anti-HER2 therapy if CTC HER2 status turned negative? Secondly, considering that some potent anti-HER2 drugs have come to the clinic [28, 38–40], whether tissue HER2 negative patients could benefit from anti-HER2 therapy when positive HER2 status in CTC was acquired? Several clinical trials have been conducted to address these questions, such as TREAT-CTC, CirCe T-DM, etc. [25, 30]. In our research cohort, the CTC number is in the range of 0–55 per 5 ml blood (Average = 7.55, Medium = 6, IQR: 3 ~ 9.6), which represents a significant improvement over studies based on Cellsearch platform (medium = 3) [41]. Although it is not based on the same patient's control, combined with cell line experiments results, we assume our system is expected

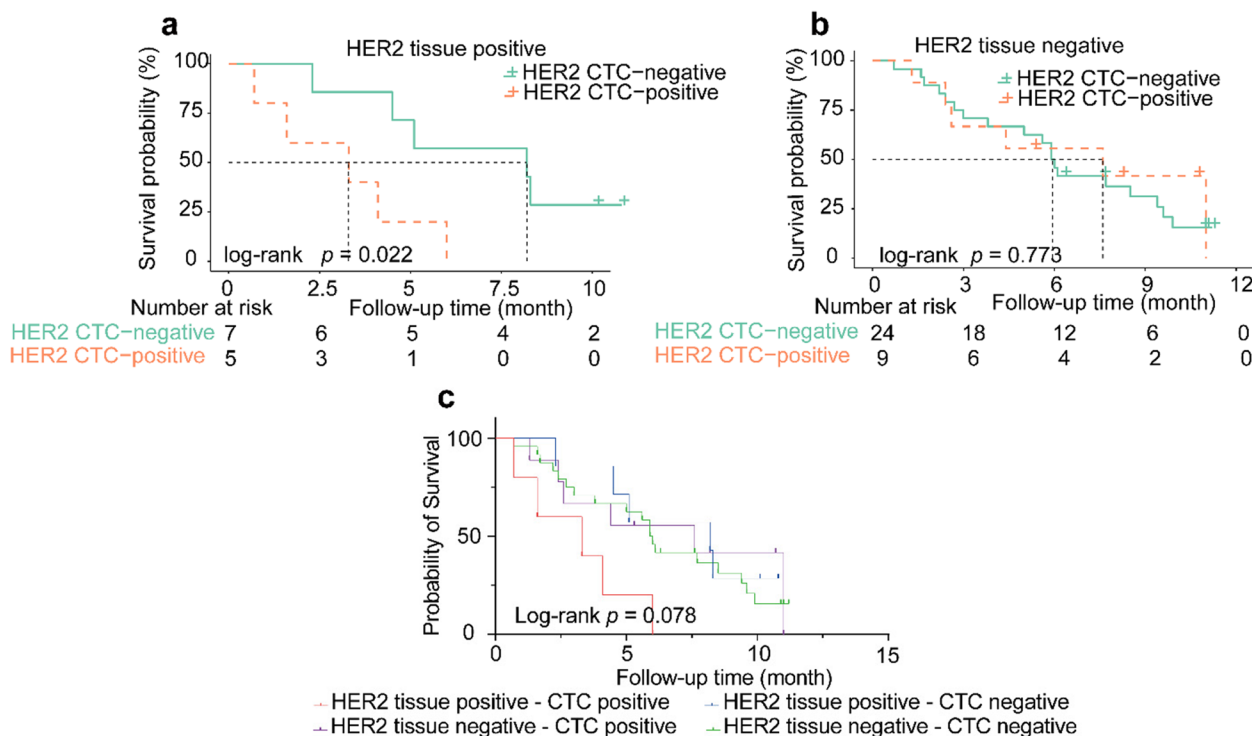


**Fig. 6** Progression-free survival (PFS) according to HER2 status on CTCs in HER2-positive MBC **(a)** and HER2-negative MBC **(b)**. Kaplan–Meier PFS estimates for combinations of HER2 status between metastatic tumor and corresponding CTCs **(c)**. Patients with HER2 tissue-positive & CTC-positive had shorter PFS than others ( $p = 0.078$ )

to improve the accuracy of CTC-HER2 characterization based on the enhancement of CTC capture efficiency and accuracy of image analysis algorithm.

In this study, we also investigated the HER2 status discordance between metastatic tumor and its corresponding CTCs and its correlation to clinical prognosis. We found that patients with positive HER2 status in both tissue and CTC had worse prognosis than that with positive tHER2 but negative cHER2 status. This observation suggests that cHER2 positive status may reflect resistance to anti-HER2 therapy in patients with tHER2 positive, resulting in the failure of eliminating HER2 positive tumor cells. A similar study reported by Jordan NV et al. has found that CTCs from HER2 negative MBC patients can exhibit HER2 positive status, these HER2 positive CTCs are more proliferative but not addicted to HER2, consistent with activation of multiple signaling pathways [22]. Patients with HER2-positive metastatic tumors in this study were treated with anti-HER2 therapy, and it is possible that activation of multiple signaling pathways may have occurred in HER2-positive CTC patients, resulting in insensitivity to anti-HER2 therapy. Conversely, in our cohort, the cHER2 status did not correlated with PFS in patients with negative tHER2. The DETECT III Clinical Trial showed that phenotyping

of CTCs might have clinical utility for stratification of MBC cancer patients to HER2-targeting therapies [42]. In this setting, CTC-HER2 status might have the potential to serve as a biomarker that predictive of patients benefiting from these novel antibody–drug conjugate (ADC) drugs with both HER2-low tumors or HER2 positive tumors that are resistant to other anti-HER2 therapies.

There were several limitations which should be considered while interpreting the study findings. First, the key limitations of the present study concern its single-center nature and a small sample size, which restricted our analysis for the subgroup based on CTCs and HER2 status. Second, longer follow-up will be required to confirm the results that associated with long-term survival. Furthermore, the various treatment regimens of MBC may affect PFS. Different blood sample collection times were another issue. Finally, a possible limitation of our study is that HER2-positivity was not scored quantitatively, the cut-off for a CTC-HER2 positive patient was defined by > 50% of CTCs detected in 5 ml blood over-expressing HER2. Moreover, the assessment of the optimum cut-off value to define an MBC patient as CTC-HER2 positive or CTC-HER2 negative is still a debated issue. Hence, randomized multicenter clinical trials with larger cohorts

and a standardized protocol are warranted to validate the finding of this research.

## Conclusion

In conclusion, the OmiCell<sup>®</sup> system, benefiting from a special type of filter and filter integration device, is a highly sensitive platform for automatic CTC detection of multi samples. Together with the DeepSight<sup>®</sup> system, the whole process of filtration-based CTC analyses become robust and standardized, thereby holding a high potential in clinical research and future applications. Our results on CTC enumeration and subsequent evaluation of HER2 status provided significant information in MBC, suggesting a higher prognostic value than that suggested with the CellSearch system. In addition, we found that the HER2 expression in CTCs was not always correlated to the HER2 expression in tumor tissues, in agreement with the previously reports. Finally, the clinical value of CTC HER2 status is worth for further investigation in order to achieve a clinical significance.

## Supplementary Information

The online version contains supplementary material available at <https://doi.org/10.1186/s12885-024-12818-1>.

Supplementary Material 1.

## Acknowledgements

We thank Wei Zhou for the system architecture design and Rui Liu for the manufacturing of membrane and integrated microfluidic chip.

## Authors' contributions

Conception and design of the study: FY, ML, CH, RXH; Acquisition of clinical data: LYW, RXH, SMS; CTC detection and HER2 evaluation: CH, YC; Analysis and interpretation of the data: LYW, RXH, CH, ML, FY; Manuscript drafting and revision: LYW, RXH, SMS, SSW, YC, CH, ML, FY. All authors read and approved the final manuscript.

## Funding

The research was supported by Natural Science Foundation of Guangdong Province (2023A1515030092), the National Natural Science Foundation of China (82372590), the Beijing Kechuang Medical Development Foundation (KC2022-ZZ-0091-3), and the Guangdong Basic and Applied Basic Research Foundation (2021B1515230010).

## Availability of data and materials

The datasets used and analyzed during the current study are available from the corresponding author on reasonable request.

## Declarations

### Ethics approval and consent to participate

Study protocols were approved by the ethical committee of Sun Yat-Sen University Cancer Center and written informed consent was obtained from all participants involved in this study (Ethics Approval ID: B2021-062). All procedures in this study were conducted in accordance with ethical principles.

### Consent for publication

Not required.

## Competing interests

Chao Han has financial interests in AnFang Biotech. All other authors declare that they have no competing interests.

## Author details

<sup>1</sup>Department of Medical Oncology, State Key Laboratory of Oncology in South China, Collaborative Innovation Center for Cancer Medicine, Sun Yat-Sen University Cancer Center, Guangzhou, China. <sup>2</sup>Department of Breast Surgery, State Key Laboratory of Oncology in South China, Collaborative Innovation Center for Cancer Medicine, Sun Yat-Sen University Cancer Center, Dongfengdong Road 651, Guangzhou 510060, China. <sup>3</sup>Department of Pathology Department, State Key Laboratory of Oncology in South China, Collaborative Innovation Center for Cancer Medicine, Sun Yat-Sen University Cancer Center, Dongfengdong Road 651, Guangzhou 510060, China. <sup>4</sup>Department of Oncology, the First Affiliated Hospital of Zhengzhou University, No.1 Eastern Jianshe Road, Zhengzhou, Henan 450052, China. <sup>5</sup>Anfang Biotechnology Co, Guanzhou Life&Science Center, LtdBio-Island, Guangzhou 510120, China. <sup>6</sup>PASTEUR, Département de Chimie, École Normale Supérieure, PSL University, CNRS, Sorbonne Université, Paris 75005, France.

Received: 18 February 2024 Accepted: 16 August 2024

Published online: 29 August 2024

## References

- Hosseini H, Obradovic MMS, Hoffmann M, et al. Early dissemination seeds metastasis in breast cancer[J]. *Nature*. 2016;540(7634):552–8.
- Alemzadeh E, Allahqoli L, Dehghan H, et al. Circulating tumor cells and circulating tumor DNA in breast cancer diagnosis and monitoring[J]. *Oncol Res*. 2023;31(5):667–75.
- Lone SN, Nisar S, Masoodi T, et al. Liquid biopsy: a step closer to transform diagnosis, prognosis and future of cancer treatments[J]. *Mol Cancer*. 2022;21(1):79.
- Riethdorf S, O'flaherty L, Hille C, et al. Clinical applications of the CellSearch platform in cancer patients. *Adv Drug Deliv Rev*. 2018;125:102–21.
- Lopes C, Piai P, Chicharo A, et al. HER2 Expression in Circulating Tumour Cells Isolated from Metastatic Breast Cancer Patients Using a Size-Based Microfluidic Device. *Cancers (Basel)*. 2021;13(17):4446.
- Yu M, Bardia A, Wittner BS, et al. Circulating breast tumor cells exhibit dynamic changes in epithelial and mesenchymal composition[J]. *Science*. 2013;339(6119):580–4.
- Chen L, Peng M, Li N, et al. Combined use of EpCAM and FRalpha enables the high-efficiency capture of circulating tumor cells in non-small cell lung cancer[J]. *Sci Rep*. 2018;8(1):1188.
- Broersen LH, Van Pelt GW, Tollenaar RA, et al. Clinical application of circulating tumor cells in breast cancer[J]. *Cell Oncol (Dordr)*. 2014;37(1):9–15.
- Ma YC, Wang L, Yu FL. Recent advances and prospects in the isolation by size of epithelial tumor cells (SET) methodology[J]. *Technol Cancer Res Treat*. 2013;12(4):295–309.
- Zhang W, Kai K, Choi DS, et al. Microfluidics separation reveals the stem-cell-like deformability of tumor-initiating cells[J]. *Proc Natl Acad Sci U S A*. 2012;109(46):18707–12.
- Balic M, Dandachi N, Hofmann G, et al. Comparison of two methods for enumerating circulating tumor cells in carcinoma patients[J]. *Cytometry B Clin Cytom*. 2005;68(1):25–30.
- Aghaamoo M, Aghilinejad A, Chen X, et al. On the design of deterministic dielectrophoresis for continuous separation of circulating tumor cells from peripheral blood cells[J]. *Electrophoresis*. 2019;40(10):1486–93.
- Alix-Panabieres C, Pantel K. Clinical Applications of Circulating Tumor Cells and Circulating Tumor DNA as Liquid Biopsy[J]. *Cancer Discov*. 2016;6(5):479–91.
- Van Der Toom EE, Verdone JE, Gorin MA, et al. Technical challenges in the isolation and analysis of circulating tumor cells[J]. *Oncotarget*. 2016;7(38):62754–66.
- Shields CWT, Reyes CD, Lopez GP. Microfluidic cell sorting: a review of the advances in the separation of cells from debulking to rare cell isolation[J]. *Lab Chip*. 2015;15(5):1230–49.

16. Lin Z, Luo G, Du W, et al. Recent Advances in Microfluidic Platforms Applied in Cancer Metastasis: Circulating Tumor Cells (CTCs) Isolation and Tumor-On-A-Chip[J]. *Small*. 2020;16(9):e1903899.
17. Tang Y, Shi J, Li S, et al. Microfluidic device with integrated microfilter of conical-shaped holes for high efficiency and high purity capture of circulating tumor cells[J]. *Sci Rep*. 2014;4:6052.
18. Woo HJ, Kim SH, Kang HJ, et al. Continuous centrifugal microfluidics (CCM) isolates heterogeneous circulating tumor cells via full automation[J]. *Theranostics*. 2022;12(8):3676–89.
19. Turner NH, Di Leo A. HER2 discordance between primary and metastatic breast cancer: assessing the clinical impact[J]. *Cancer Treat Rev*. 2013;39(8):947–57.
20. Cejalvo JM, Martinez De Duenas E, Galvan P, et al. Intrinsic Subtypes and Gene Expression Profiles in Primary and Metastatic Breast Cancer. *Cancer Res*. 2017;77(9):2213–21.
21. Aktas B, Kasimir-Bauer S, Muller V, et al. Comparison of the HER2, estrogen and progesterone receptor expression profile of primary tumor, metastases and circulating tumor cells in metastatic breast cancer patients[J]. *BMC Cancer*. 2016;16:522.
22. Jordan NV, Bardia A, Wittner BS, et al. HER2 expression identifies dynamic functional states within circulating breast cancer cells[J]. *Nature*. 2016;537(7618):102–6.
23. Ignatiadis M, Rothe F, Chaboteaux C, et al. HER2-positive circulating tumor cells in breast cancer[J]. *PLoS ONE*. 2011;6(1):e15624.
24. Fehm T, Muller V, Aktas B, et al. HER2 status of circulating tumor cells in patients with metastatic breast cancer: a prospective, multicenter trial[J]. *Breast Cancer Res Treat*. 2010;124(2):403–12.
25. Jacot W, Cottu P, Berger F, et al. Actionability of HER2-amplified circulating tumor cells in HER2-negative metastatic breast cancer: the CirCe T-DM1 trial[J]. *Breast Cancer Res*. 2019;21(1):121.
26. Pestrin M, Bessi S, Galardi F, et al. Correlation of HER2 status between primary tumors and corresponding circulating tumor cells in advanced breast cancer patients[J]. *Breast Cancer Res Treat*. 2009;118(3):523–30.
27. Riethdorf S, Muller V, Zhang L, et al. Detection and HER2 expression of circulating tumor cells: prospective monitoring in breast cancer patients treated in the neoadjuvant GeparQuattro trial[J]. *Clin Cancer Res*. 2010;16(9):2634–45.
28. Wang C, Mu Z, Ye Z, et al. Prognostic value of HER2 status on circulating tumor cells in advanced-stage breast cancer patients with HER2-negative tumors[J]. *Breast Cancer Res Treat*. 2020;181(3):679–89.
29. Jaeger BAS, Neugebauer J, Andergassen U, et al. The HER2 phenotype of circulating tumor cells in HER2-positive early breast cancer: A translational research project of a prospective randomized phase III trial. *PLoS One*. 2017;12(6):e0173593.
30. Pestrin M, Bessi S, Puglisi F, et al. Final results of a multicenter phase II clinical trial evaluating the activity of single-agent lapatinib in patients with HER2-negative metastatic breast cancer and HER2-positive circulating tumor cells. A proof-of-concept study. *Breast Cancer Res Treat*. 2012;134(1):283–9.
31. Deutsch TM, Riethdorf S, Fremd C, et al. HER2-targeted therapy influences CTC status in metastatic breast cancer[J]. *Breast Cancer Res Treat*. 2020;182(1):127–36.
32. Ayyachamy S, Alex V, Khened M, Krishnamurthi G. Medical image retrieval using Resnet-18 for clinical diagnosis. *Medical Imaging 2019: Imaging Informatics for Healthcare, Research, and Applications*. 2019;10954:1095410–9. <https://doi.org/10.1117/12.2515588>.
33. Pantel K, Brakenhoff RH, Brandt B. Detection, clinical relevance and specific biological properties of disseminating tumour cells[J]. *Nat Rev Cancer*. 2008;8(5):329–40.
34. Gordian-Arroyo AM, Zynger DL, Tozbikian GH. Impact of the 2018 ASCO/CAP HER2 Guideline Focused Update[J]. *Am J Clin Pathol*. 2019;152(1):17–26.
35. Templeman A, Miller MC, Cooke MJ, et al. Analytical performance of the FDA-cleared Parsortix((R)) PC1 system[J]. *J Circ Biomark*. 2023;12:26–33.
36. Cristofanilli M, Budd GT, Ellis MJ, et al. Circulating tumor cells, disease progression, and survival in metastatic breast cancer[J]. *N Engl J Med*. 2004;351(8):781–91.
37. Carlsson J, Nordgren H, Sjostrom J, et al. HER2 expression in breast cancer primary tumours and corresponding metastases. Original data and literature review. *Br J Cancer*. 2004;90(12):2344–8.
38. Modi S, Saura C, Yamashita T, et al. Trastuzumab Deruxtecan in Previously Treated HER2-Positive Breast Cancer[J]. *N Engl J Med*. 2020;382(7):610–21.
39. Menderes G, Bonazzoli E, Bellone S, et al. SYD985, a Novel Duocarmycin-Based HER2-Targeting Antibody-Drug Conjugate, Shows Antitumor Activity in Uterine and Ovarian Carcinosarcoma with HER2/Neu Expression[J]. *Clin Cancer Res*. 2017;23(19):5836–45.
40. Hong R, Xia W, Wang L, et al. Safety, tolerability, and pharmacokinetics of BAT8001 in patients with HER2-positive breast cancer: An open-label, dose-escalation, phase I study[J]. *Cancer Commun (Lond)*. 2021;41(2):171–82.
41. Banys-Paluchowski M, Krawczyk N, Fehm T. Potential Role of Circulating Tumor Cell Detection and Monitoring in Breast Cancer: A Review of Current Evidence[J]. *Front Oncol*. 2016;6:255.
42. Fehm T, Mueller V, Banys-Paluchowski M, et al. Efficacy of Lapatinib in Patients with HER2-Negative Metastatic Breast Cancer and HER2-Positive Circulating Tumor Cells-The DETECT III Clinical Trial[J]. *Clin Chem*. 2024;70(1):307–18.

### Publisher's Note

Springer Nature remains neutral with regard to jurisdictional claims in published maps and institutional affiliations.